Am J Physiol Heart Circ Physiol 304: H916–H926, 2013.
First published February 1, 2013; doi:10.1152/ajpheart.00026.2012.

CALL FOR PAPERS | *Mitochondria in Cardiovascular Physiology and Disease*

Glutathione oxidation unmasks proarrhythmic vulnerability of chronically hyperglycemic guinea pigs

Chaoqin Xie,[1] Nora Biary,[1] Carlo G. Tocchetti,[2] Miguel A. Aon,[2] Nazareno Paolocci,[2] Justin Kauffman,[1] and Fadi G. Akar[1]

[1]*Cardiovascular Institute, Mount Sinai School of Medicine, New York, New York; and* [2]*Division of Cardiology, Johns Hopkins University, Baltimore, Maryland*

Submitted 12 January 2012; accepted in final form 25 January 2013

Xie C, Biary N, Tocchetti CG, Aon MA, Paolocci N, Kauffman J, Akar FG. Glutathione oxidation unmasks proarrhythmic vulnerability of chronically hyperglycemic guinea pigs. *Am J Physiol Heart Circ Physiol* 304: H916–H926, 2013. First published February 1, 2013; doi:10.1152/ajpheart.00026.2012.—Chronic hyperglycemia in type-1 diabetes mellitus is associated with oxidative stress (OS) and sudden death. Mechanistic links remain unclear. We investigated changes in electrophysiological (EP) properties in a model of chronic hyperglycemia before and after challenge with OS by GSH oxidation and tested reversibility of EP remodeling by insulin. Guinea pigs survived for 1 mo following streptozotocin (STZ) or saline (sham) injection. A treatment group received daily insulin for 2 wk to reverse STZ-induced hyperglycemia (STZ + Ins). EP properties were measured using high-resolution optical action potential mapping before and after challenge of hearts with diamide. Despite elevation of glucose levels in STZ compared with sham-operated ($P = 0.004$) and STZ + Ins ($P = 0.002$) animals, average action potential duration (APD) and arrhythmia propensity were not altered at baseline. Diamide promoted early (<10 min) formation of arrhythmic triggers reflected by a higher arrhythmia scoring index in STZ ($P = 0.045$) and STZ + Ins ($P = 0.033$) hearts compared with sham-operated hearts. APD heterogeneity underwent a more pronounced increase in response to diamide in STZ and STZ + Ins hearts compared with sham-operated hearts. Within 30 min, diamide resulted in spontaneous incidence of ventricular tachycardia and ventricular fibrillation (VT/VF) in 3/6, 2/5, 1/5, and 0/4 STZ, STZ + Ins, sham-operated, and normal hearts, respectively. Hearts prone to VT/VF exhibited greater APD heterogeneity ($P = 0.010$) compared with their VT/VF-free counterparts. Finally, altered EP properties in STZ were not rescued by insulin. In conclusion, GSH oxidation enhances APD heterogeneity and increases arrhythmia scoring index in a guinea pig model of chronic hyperglycemia. Despite normalization of glycemic levels by insulin, these proarrhythmic properties are not reversed, suggesting the importance of targeting antioxidant defenses for arrhythmia suppression.

type-1 diabetes mellitus; insulin; oxidative stress; electrical remodeling; conduction; repolarization; arrhythmias

PATIENTS WITH type-1 diabetes mellitus (t1DM) are at a heightened risk of sudden cardiac death (29). Increased mortality in these patients is attributable to a variety of cardiovascular complications including atherosclerosis, ischemic injury, and myocardial infarction, all of which are important risk factors for ventricular arrhythmias (8). Growing evidence implicates oxidative stress (OS) in general and glutathione (GSH) depletion, in particular in the pathophysiology of t1DM (13a, 25a, 34, 42). Whether OS is a required component of the arrhythmia substrate of the diabetic heart is unknown.

Previous studies of arrhythmia mechanisms in t1DM hearts have extensively focused on ion channel remodeling at the isolated myocyte level (25, 40, 45, 46). Several studies identified prolongation of the action potential duration (APD) as an important electrophysiological (EP) signature of myocytes from diabetic hearts (25, 46). Because APD and QT-interval prolongation promote early afterdepolarization-mediated triggers and polymorphic ventricular tachycardia and ventricular fibrillation (VT/VF) in acquired and congenital forms of the long QT syndrome and heart failure, it was proposed that APD prolongation in t1DM may also be arrhythmogenic. In support of this idea is the fact that QT-interval prolongation has emerged as an important risk factor for mortality in patients with t1DM (11).

On the other hand, cellular EP studies in t1DM were mostly performed in small rodents (mice and rats) whose AP profile lacks a plateau phase and whose rapid repolarization kinetics are governed almost exclusively by the transient outward K^+ current (I_{to}) (6, 19, 26, 31, 38–40, 46). In contrast, guinea pigs and larger mammalian species, including humans, exhibit action potentials that have a prominent plateau phase and that display gradual repolarization kinetics that are not strictly dependent on I_{to}. Rather, terminal repolarization and APD in these species reflect a delicate balance in the activation and inactivation properties of multiple ionic currents, including the delayed rectifier K^+ currents, the sodium-calcium exchanger, the L-type calcium current, and the inward rectifier K^+ current. This distinction is important because unlike rodents, patients with t1DM do not exhibit heart rate corrected QT-interval prolongation in the absence of confounding factors, such as diabetic ketoacidosis (24) or spontaneous hypoglycemia (11). Clinically, these additional stimuli are required to unmask pathological QT-interval prolongation in patients with t1DM (11, 14, 17, 24).

More importantly, most EP studies in t1DM have been performed in animal models that exhibited highly artificial rises (>300%) in blood glucose levels that are well beyond what is commonly encountered in patients with diabetes (20, 33, 36, 40, 46). Such extreme levels of hyperglycemia, which are known to affect ion channels, preclude the direct translation of some of these earlier findings to humans. Therefore, a major objective of the present study was to create a robust and reproducible animal model of chronic hyperglycemia that ex-

Address for reprint requests and other correspondence: F. G. Akar, Cardiovascular Inst., Mount Sinai School of Medicine, 1 Gustave L. Levy Pl., New York, NY 10029 (e-mail: fadi.akar@mssm.edu).

hibits qualitatively similar elevations in plasma glucose levels, as found in humans (i.e., by ~25–50%), and in which EP properties could be related directly to arrhythmia propensity. Specifically, we performed a comprehensive investigation of the tissue-level EP substrate in a guinea pig model of streptozotocin (STZ)-induced hyperglycemia and investigated for the first time the potential reversibility of EP remodeling by chronic insulin treatment. Finally, because GSH depletion is central to the pathophysiology of t1DM (13a, 25a, 34, 42), we hypothesized that GSH oxidation using diamide may unmask functionally important differences in EP properties and promote arrhythmias in chronic hyperglycemia.

METHODS

Experimental Models of Chronic Hyperglycemia With and Without Chronic Insulin Treatment

Procedures involving the handling of animals were approved by the Animal Care and Use Committee and adhered with the *Guide for the Care and Use of Laboratory Animals*, published by the National Institutes of Health (NIH publication No. 85-23, Revised 1996). Experimental models of chronic hyperglycemia with and without insulin treatment were prepared at Hilltop Lab Animals (Scottdale, PA) according to a protocol designed for this study (Fig. 1*A*). Briefly, adult male Hartley guinea pigs were allowed to survive for 1 mo following a single intraperitoneal injection (80 mg/kg in citrate buffer) of buffered STZ ($n = 11$) or an equivalent volume of citrate-buffered saline (sham, $n = 10$). A treatment group ($n = 6$) received 1 U/day insulin glargine (Lantus, Aventis) by subcutaneous injection for an additional 2 wk following onset of hyperglycemia by STZ injection (STZ + Ins). A group of eight normal guinea pigs was used to establish the protocol of acute OS by diamide perfusion (Fig. 1, *B* and *C*). Before animal death, blood glucose levels were measured three to five times per animal using the clarity plus glucometer (Diagnostic Test Group, Boca Raton, FL). The in vivo protocol used to induce hyperglycemia resulted in a significant elevation in plasma glucose levels, which is comparable (on a percent basis) with what is observed in patients with t1DM (Fig. 2*A*).

Ex Vivo Optical Action Potential Mapping

Following assessment of plasma glucose levels, guinea pigs ($n = 26$) were anesthetized and their hearts were rapidly excised and retrogradely perfused via the aorta with oxygenized (95% O_2-5% CO_2) Tyrode solution containing (in mM) 130 NaCl, 1.2 $MgSO_4$, 25 $NaHCO_3$, 4.75 KCl, 5 dextrose, and 1.25 $CaCl_2$ at 36.5 ± 1°C. Both atria were surgically removed to avoid competitive stimulation of the ventricles by the sinoatrial node. Perfusion pressure was maintained at ~60–70 mmHg by adjusting the perfusion flow rate.

Hearts were positioned in a custom-built chamber with their anterior surface gently pressed against a glass imaging window by a customized U-shaped piston, as described in detail elsewhere (21, 28). Movement was suppressed using 10 μM blebbistatin (Tocris Bioscience) mixed in Tyrode solution for 10 min. Preparations were immersed in the coronary effluent to maintain temperature at 36 ± 1°C. Volume-conducted electrocardiograms (ECG) were recorded for cardiac rhythm monitoring, analysis, and arrhythmia scoring using noncontact silver electrodes. ECG signals were amplified using the ECG100-MP150 amplifier system and the *Acqknowledge* 3.9 software package (Biopac System, Goleta, CA).

After stabilizing for 10 min, hearts were stained with 20 μM of the voltage-sensitive dye di-4-ANEPPS (Invitrogen) mixed in Tyrode solution for 10 min. Hearts were excited with filtered light (515 ± 5 nm) from a high-power, low-noise quartz tungsten halogen lamp (Newport, CT). The emitted fluorescence was filtered (>620 nm) and focused onto a high-resolution, 80 × 80-pixel CCD camera (SciMeasure) that was

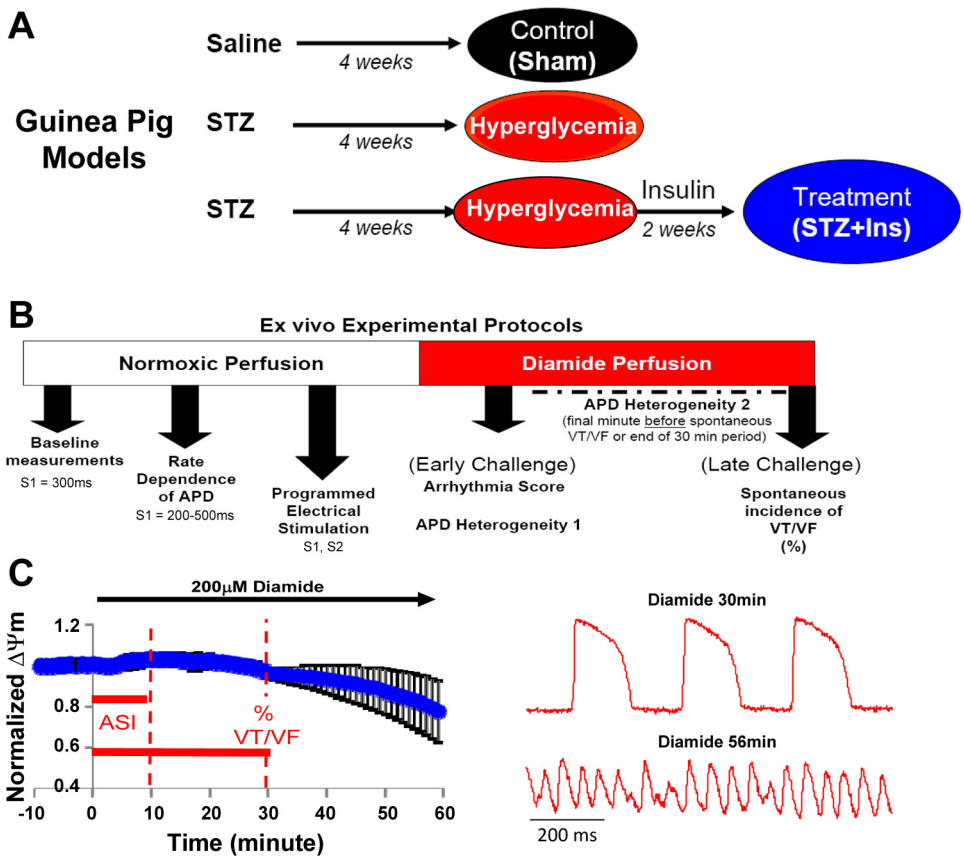

Fig. 1. In vivo and ex vivo experimental models and protocols. *A*: development of guinea pig models of streptozotocin-induced hyperglycemia with (STZ + Ins) and without (STZ) chronic insulin treatment. *B*: ex vivo experimental protocols used to determine electrophysiological properties. *C*: Diamide-induced changes in mitochondrial and electrical properties in normal guinea pig hearts, indicating stable membrane potential ($\Delta\Psi_m$; *left*) and action potential (*right*) properties during the initial 30-min period of challenge. These measurements guided the ex vivo electrophysiological protocol used in sham-operated, STZ, and STZ + Ins groups, in which we focused on this 30-min window. APD, action potential duration; VT/VF, ventricular tachycardia and ventricular fibrillation; ASI, arrhythmia scoring index.

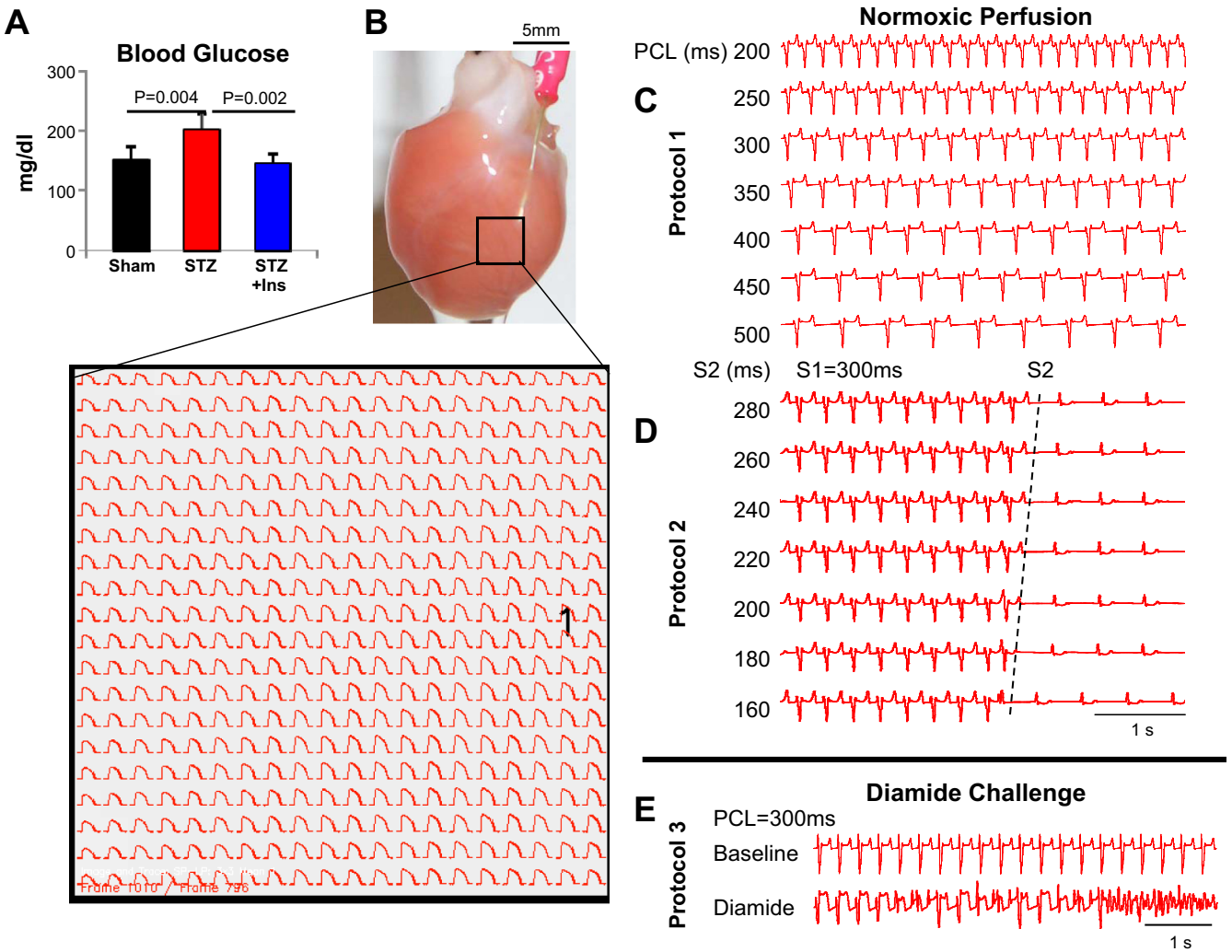

Fig. 2. Animal models of STZ + Ins and STZ. *A*: average blood glucose levels in sham-operated (saline injected), STZ, and STZ + Ins animals. *B*: ex vivo perfused guinea pig heart indicating approximate location and size of the mapping field on the left ventricular epicardium. Also shown are representative simultaneously recorded action potentials from across the 4 × 4-mm^2 region. *C* and *D*: ex vivo experimental protocols. *C*: *protocol 1*, representative volume conducted ECG traces recorded during steady-state pacing at a wide range of pacing cycle lengths (PCLs; 200–500 ms). *D*: *protocol 2*, programmed electrical stimulation using a single premature extra-stimulus delivered at decreasing coupling intervals until arrhythmias were produced or refractoriness encountered. *E*: *protocol 3*, arrhythmia propensity by challenge with oxidative stress produced by GSH oxidation (perfusion with 200 μM diamide).

coupled to an imaging macroscope containing a modular high-numerical aperture lens, a dichroic mirror, excitation and emission filters, a beam splitter, and a light collimating tube.

During each recording, 6,400 independent action potentials were simultaneously imaged from a 4 × 4-mm^2 region of the left ventricular (LV) epicardium (Fig. 2*B*) yielding an inter-pixel resolution of 50 μm × 50 μm. To further improve signal quality, a 4 × 4 digital binning filter was applied to the raw signals, thereby reducing the effective spatial resolution to 200 μm × 200 μm. As illustrated in Fig. 1*B*, this strategy allowed the accurate detection of activation and repolarization times from all action potentials across the mapping field (Fig. 2*B*).

Ex Vivo Experimental Protocols

Normoxic perfusion. Each heart was subjected to an identical set of experimental protocols (Fig. 1*B*). Initially, hearts were perfused with normal Tyrode solution. Following assessment of baseline EP properties, hearts were paced at multiple cycle lengths ranging from 200 to 500 ms, as illustrated in Fig. 2. Using this protocol, we investigated the rate dependence of EP properties in hearts from sham-operated, STZ, and STZ + Ins animals.

Hearts were then challenged with an ex vivo programmed electrical stimulation (PES) protocol, which entailed delivery of premature impulses (S2) at decreasing coupling intervals (in 20-ms decrements) relative to the pacing (S1) train (cycle length, 300 ms) until refractoriness was encountered or an arrhythmia induced (Fig. 2*D*). APD restitution defined as the APD dependence of the premature (S2) beat on the previous S1S2 coupling interval was assessed. Stimuli were delivered using a silver electrode placed on the anterior LV surface (Fig. 2*B*). The stimulus strength was set to two times the diastolic pacing threshold at a pulse width of 2 ms.

Diamide perfusion. Since none of the hearts exhibited arrhythmias during normoxic perfusion (see Results), hearts were challenged with a reliable ex vivo protocol of OS by diamide (200 μM) perfusion, which produces mitochondrial and electrical dysfunction (9). We focused on the initial 30-min period of diamide perfusion, because in preliminary experiments, we found that normal hearts remained electrically and metabolically stable during that time course (Fig. 1*C*).

Sensitivity to OS challenge was quantified in sham-operated, STZ, and STZ + Ins hearts upon early (10 min) exposure to diamide using an arrhythmia scoring index (ASI), which reflects the presence and severity of arrhythmic triggers. Detailed measurements of APD heterogeneity across the mapping field were performed for paced beats following 10 min of diamide perfusion in all hearts (early challenge).

Diamide perfusion was sustained for 30 min in all hearts to assess the spontaneous induction rate of VT/VF. Measurements of APD heterogeneity were repeated for paced beats following 30 min of diamide challenge in VT/VF (−) hearts or during the last minute of successful pacing before onset of arrhythmias in VT/VF (+) hearts. This allowed us to compare APD heterogeneity in VT/VF (−) versus VT/VF (+) hearts. Although guinea pig preparations are stable for over 4 h of ex vivo perfusion, all experimental protocols were completed within 2.5 h of animal death.

EP Measurements

Action potential duration. APD was defined as the difference between repolarization and activation times for each recorded action potential. Activation time was defined as the maximum first derivative during the action potential upstroke, whereas repolarization time was defined as the point of maximum second derivative during the repolarization phase at each site. APD values were measured during steady-state pacing before and after challenge with diamide and immediately (within 1 min) before onset of spontaneous arrhythmias.

APD heterogeneity. APD heterogeneity was quantified as the standard deviation (SD-APD) or range (R-APD) of APD values measured over a 4×4-mm^2 region of the LV epicardium. SD-APD and R-APD were measured in all hearts during steady-state pacing before and after challenge with diamide. APD heterogeneity was first measured following 10 min of diamide treatment. APD heterogeneity was also measured before spontaneous onset of arrhythmias by diamide in VT/VF (+) hearts or at the end of the 30-min diamide protocol in VT/VF (−) hearts.

Conduction velocity. Velocity vectors (magnitude and direction) were derived from the activation times of each pixel relative to those of its neighbors. Conduction velocity (CV) was measured by averaging the magnitude of the velocity vectors along the main direction of impulse propagation.

Arrhythmia scoring index. Arrhythmia sensitivity was evaluated by using a standard ASI as we and others have previously described (7, 9, 22). Briefly, ASI was generated according to the following criteria during the initial 10-min period of diamide challenge in each heart: 0, 0 ventricular premature beats; 1, 1–10 ventricular premature beats; 2, 11–50 ventricular premature beats; 3, 51–100 ventricular premature beats; 4, 101–500 ventricular premature beats; 5, sustained VT/VF.

Statistical Analyses

EP differences between the sham-operated and experimental (STZ or STZ + Ins) groups were compared using one-way ANOVA with Tukey's post hoc analysis in SPSS. Differences were considered significant for $P < 0.05$. Student's *t*-test was used to compare differences in APD heterogeneity between VT/VF (+) and VT/VF (−) hearts.

RESULTS

A New Model of Chronic Hyperglycemia in Guinea Pigs

Shown in Fig. 2*A* are average blood glucose levels in sham-operated, STZ, and STZ + Ins animals before death. Clearly, STZ injection produced a significant elevation (by 33.9%, $P < 0.004$) in plasma glucose levels compared with saline-injected controls (sham). Importantly, hyperglycemia in this guinea pig model was completely reversed by a 2-wk regimen of daily insulin treatment (Fig. 2*A*, blue). Indeed, blood glucose levels were comparable [P = not significant (NS)] between STZ + Ins and sham-operated animals. Following assessment of in vivo blood glucose levels in all groups, animals were euthanized and hearts rapidly excised, cannulated, perfused, and stained for optical action potential mapping studies (Fig. 2*B*). A detailed assessment of the EP substrate and risk of arrhythmias was performed during challenge with various ex vivo experimental protocols (Fig. 2, *C–E*).

Rate Dependence of APD

Several studies have reported APD prolongation in rat models of diabetes mellitus (47). Since most of these studies were performed in isolated myocytes, the relevance of cellular APD prolongation to arrhythmia propensity in the intact heart remained untested. By and large, these measurements were also performed in models that exhibited excessive (>350%) elevations in plasma glucose levels that are well beyond what is typically observed in patients with t1DM (i.e., ~25–50%) (13, 20, 33, 46). Therefore, we began by examining whether APD prolongation is indeed a characteristic of this guinea pig model which exhibits a qualitatively similar rise (on a percent basis) in blood glucose levels, as clinically observed in patients.

Shown in Fig. 3*A* are average APD measurements obtained over a wide range (200–500 ms) of pacing cycle lengths in sham-operated (black), STZ (red), and STZ + Ins (blue) hearts. Also shown are representative action potential traces recorded at multiple pacing cycle lengths from each group (Fig. 3*B*). Surprisingly, we found no evidence of APD prolongation in this guinea pig model of STZ-induced chronic hyperglycemia, since average APD was virtually identical (P = NS) across groups at all pacing cycle lengths that were tested (Fig. 3).

Conduction Remodeling

We proceeded to investigate potential differences in conduction properties. Shown in Fig. 4 are representative depolarization isochrone maps recorded from sham-operated, STZ, and STZ + Ins hearts (Fig. 4*A*) and action potential upstrokes depicting epicardial conduction delays caused by point stimulation in these hearts (Fig. 4*B*). Also shown are average epicardial conduction velocities (Fig. 4*C*) and normalized upstroke velocity measurements (Fig. 4*D*). Clearly, CV underwent a modest (14.4%, $P = 0.048$) reduction in STZ compared with sham-operated hearts. Interestingly, insulin treatment failed to restore CV in STZ + Ins hearts to sham-operated heart values despite complete normalization of blood glucose levels. We next tested whether impaired conduction in chronic hyperglycemia was caused by reduced excitability. As shown in Fig. 4*D*, CV slowing could not be explained by a change in excitability since the average normalized upstroke velocities were not altered in STZ (P = NS) and STZ + Ins (P = NS) hearts compared with sham-operated hearts.

Arrhythmia Propensity During Baseline Perfusion

Previous studies in rodents suggested (but did not demonstrate) that EP changes; namely, APD prolongation and conduction slowing may underlie an increased susceptibility of the t1DM heart to arrhythmias. Therefore, we began by asking whether hearts from STZ-injected guinea pigs were indeed

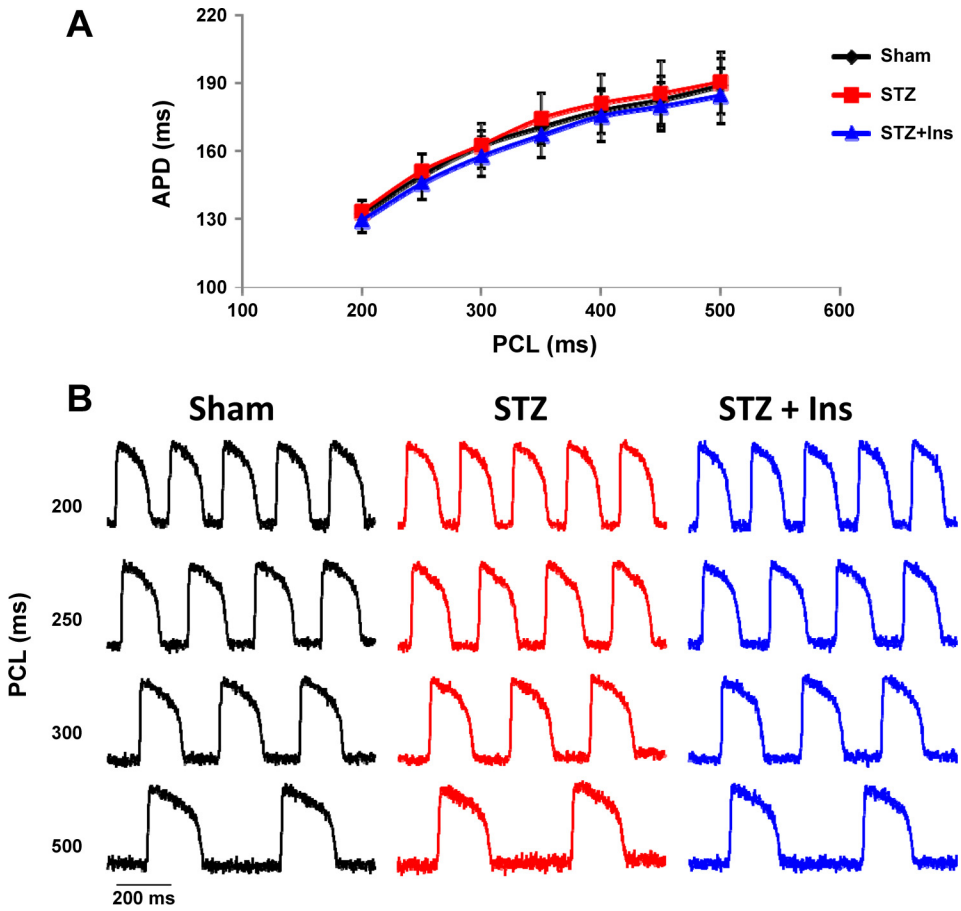

Fig. 3. Rate-dependence of APD at the tissue level. *A*: average rate dependence of APD in sham-operated (black), STZ (red), and Ins-treated (blue) animals. *B*: representative action potential traces recorded over a wide range (200–500 ms) of PCLs from each group.

more vulnerable to the incidence of arrhythmias. To address this question, we challenged hearts with an ex vivo PES protocol (Fig. 2*D*) that we had previously used to uncover heightened arrhythmia propensity in various animal models of heart disease, including heart failure and the long QT syndrome (3, 5). As shown in Fig. 5*A*, PES failed to induce arrhythmias in all groups during baseline perfusion. Moreover, a plot of the S2 APD as a function of the preceding coupling interval (S1S2) revealed similar APD restitution kinetics for sham-operated, STZ, and STZ + Ins groups (Fig. 5, *B* and *C*).

Because challenge of STZ and STZ + Ins hearts with PES failed to elicit arrhythmias, the relevance of altered EP properties remained unknown. We next hypothesized that GSH oxidation using diamide may unmask otherwise subtle differences in arrhythmia susceptibility between groups and that this strategy may identify functionally significant differences in EP properties. To that end, hearts from sham-operated, STZ, and STZ + Ins animals were challenged with 200 μM diamide. Importantly, the arrhythmic sensitivity of hearts could be quantitatively compared between groups during predefined early (10 min) and late (30 min) intervals of diamide exposure. As shown in Fig. 6*A*, diamide challenge for 10 min revealed a marked increase in ASI in STZ ($P = 0.045$) and STZ + Ins ($P = 0.033$) hearts compared with sham-operated hearts. The early rise in ASI was caused by enhanced ectopy as evidenced by presence of spontaneous action potential wave fronts emanating from multiple foci (Fig. 6*B*). These data suggest that chronically hyperglycemic animals (STZ group) are indeed more sensitive to OS-mediated arrhythmia triggers compared with controls (sham-operated group). In addition, we compared the spontaneous incidence of sustained VT/VF within a 30-min period of diamide perfusion. As shown in Figure 6*C*, there was a trend ($P = 0.13$) toward a greater incidence of VT/VF in STZ (3/6) compared with combined normal and sham-operated animals (1/9). Importantly, insulin treatment (STZ + Ins group) failed to reduce ASI (Fig. 6*A*, P = NS) and the incidence of VT/VF (Fig. 6*C*) compared with STZ alone.

Diamide-Mediated EP Properties

We proceeded to investigate differences in the EP substrate between groups during diamide challenge. Ex vivo perfusion with diamide (200 μM) caused a comparable decrease in APD in all groups (Fig. 7*A*) before arrhythmia onset. Hence, diamide-induced changes in average APD could not explain inherent differences in arrhythmia vulnerability between groups.

We next investigated potential differences in APD heterogeneity, a known mechanism of proarrhythmia in various congenital and acquired cardiovascular disorders. Shown in Fig. 7*C* are representative APD contour maps measured from sham-operated, STZ, and STZ + Ins hearts at baseline and following challenge with diamide for 10 min. Also shown are the average SD-APD and R-APD across the mapping field in all groups (Fig. 7*D*). STZ hearts were associated with significantly greater APD heterogeneity compared with sham-oper-

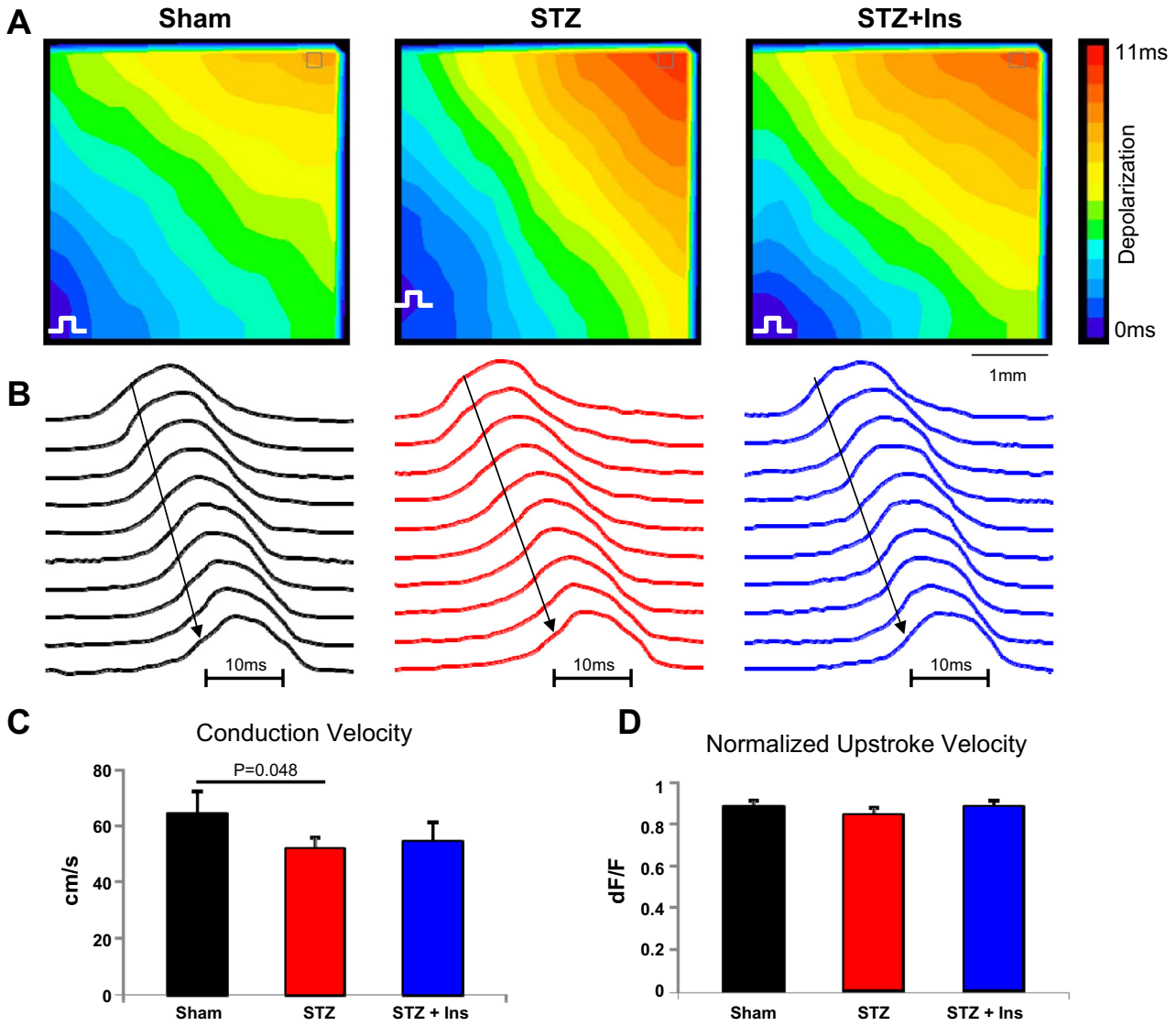

Fig. 4. Conduction remodeling in chronic hyperglycemia and its potential reversal by Ins. *A*: representative depolarization isochrone maps recorded from sham-operated, STZ, and STZ + Ins hearts. *B*: representative first derivatives of the action potential upstroke recorded simultaneously from equidistant sites of sham-operated, STZ, and STZ + Ins hearts, indicating conduction delay across the mapping field. *C*: average conduction velocity in all sham-operated (black), STZ (red), and STZ + Ins (blue) hearts. *D*: average normalized upstroke velocity as an index of cellular excitability [maximum amplitude of first derivative divided by the action potential amplitude (dF/F)] in sham-operated, STZ, and STZ + Ins hearts.

ated hearts. Interestingly, insulin treatment failed to restore SD-APD and R-APD to sham-operated levels. While challenge of hearts with diamide increased SD-APD in all groups, this effect was significantly more pronounced in the STZ (by 39.2%) and STZ + Ins (by 43.7%) groups compared with their sham-operated counterpart (by 24.3%). To further investigate the functional relevance of increased APD heterogeneity, we compared SD-APD and R-APD between hearts that were prone to (+) versus protected against (−) sustained VT/VF within a 30 min window of diamide perfusion. Remarkably, both SD-APD ($P = 0.005$) and R-APD ($P = 0.010$) were significantly higher in hearts prone to diamide-induced VT/VF (Fig. 8, *A* and *B*) compared with VT/VF free hearts.

DISCUSSION

In the present work, we set out to investigate the EP substrate in a model of STZ-induced chronic hyperglycemia and relate it directly to arrhythmia propensity. A major objective was to determine the potential reversibility of key EP changes by insulin treatment. Finally, we asked whether hyperglycemia per se is a necessary and sufficient requirement for the genesis of arrhythmias or whether additional factors, such as OS, are required to unmask inherent vulnerabilities. To do so, we developed a guinea pig model of chronic hyperglycemia in which plasma glucose elevation closely matched what is observed in patients with t1DM.

Guinea Pig Model of Chronic Hyperglycemia

The vast majority of previous studies focusing on the electrophysiology of t1DM have relied on rodent models with rapid repolarization kinetics (6, 13, 16, 31, 33, 39–41) and/or in which highly artificial rises in blood glucose levels were achieved (25, 47). In these earlier studies, APD prolongation was documented, leading to the speculation that

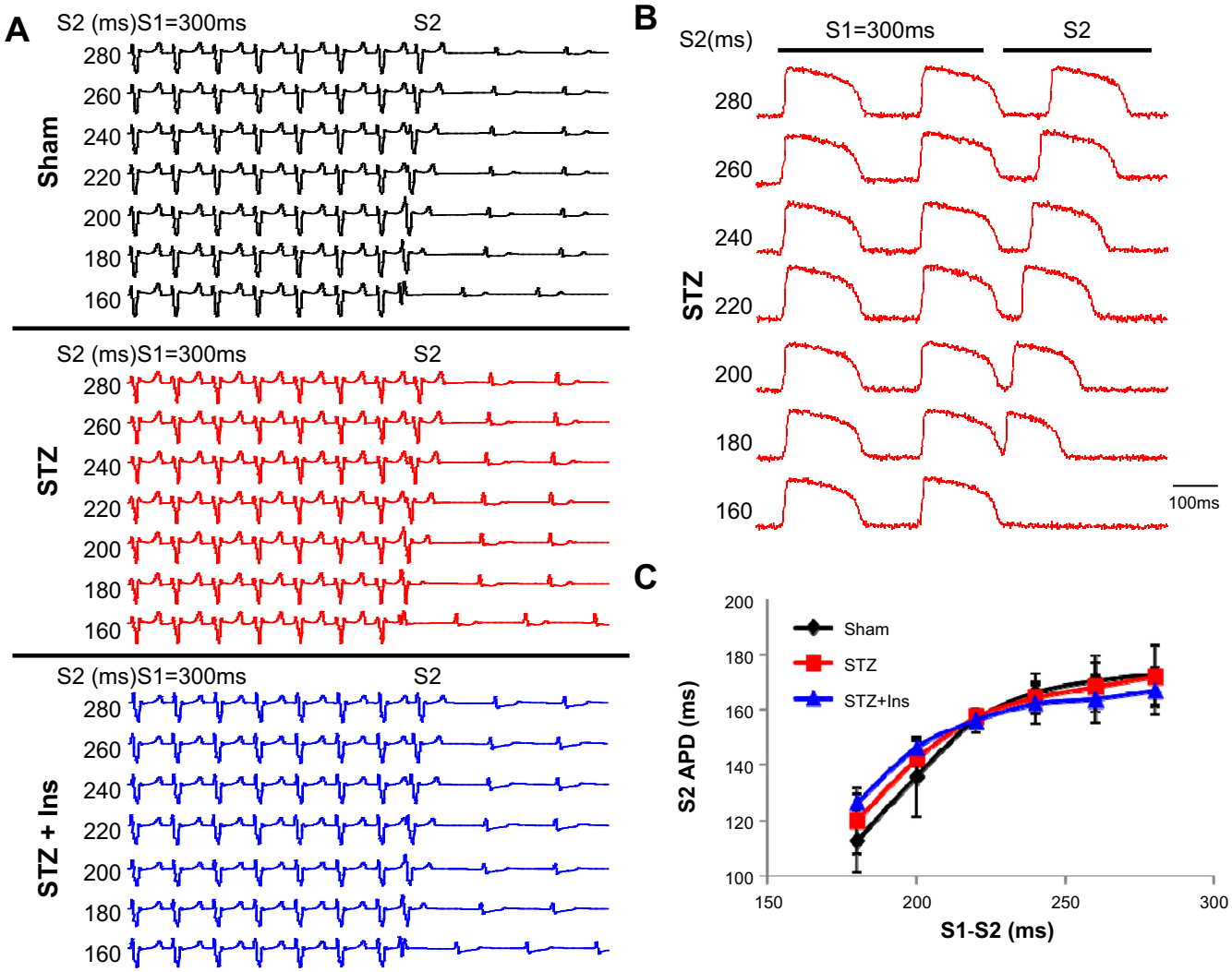

Fig. 5. Programmed electrical stimulation and restitution kinetics. *A*: representative volume-conducted ECGs from each group during challenge with programmed electrical stimulation revealing lack of arrhythmia inducibility. *B*: representative S1 and S2 action potential traces recorded before and after challenge with programmed electrical stimulation, respectively. *C*: restitution curves revealing the dependence of the S2 APD on the preceding S1S2 coupling interval in all hearts from all groups.

prolonged APD at the cellular level likely underlies QT-interval prolongation in t1DM. Since APD prolongation is a well-established arrhythmia mechanism in various models of congenital and acquired heart diseases, it was further speculated that such prolongation may underlie an enhanced susceptibility to sudden cardiac death in diabetes. A major objective of the present study was to verify the potential link between altered APD properties and arrhythmia propensity in a model of chronic hyperglycemia that exhibits a comparable rise in plasma glucose levels, as found in humans.

Surprisingly, we found that despite significant hyperglycemia, average and rate dependence of APD in guinea pigs were not altered compared with saline-injected animals (Fig. 3). Instead, hearts from STZ-injected guinea pigs were characterized by normal action potential morphologies and durations. Many factors may contribute to this apparent discrepancy. Clearly, the most obvious is the relative contribution of I_{to} to action potential repolarization across species. In rats, repolarization kinetics are almost exclusively dictated by I_{to}. Of note, Li et al. (26) have demonstrated strong redox regulation of I_{to} remodeling in the diabetic heart. In addition, slowing of I_{to} recovery from inactivation caused by a switch in the molecular component of I_{to} from Kv4.x to Kv1.4 channels has been documented in t1DM (31). Indeed, these findings may underlie the striking reduction in repolarization reserve of diabetic rats but not guinea pigs. Whereas I_{to} is expressed in humans, its contribution to terminal repolarization is relatively minimal. Indeed, our findings are qualitatively similar to those of Lengyel et al. (25) who reported a minimal (<9%) change of APD in a canine model of Alloxan-induced diabetes.

A major objective of our experimental design was the generation of an animal model that exhibits clinically relevant elevations in plasma glucose levels while avoiding other confounding factors such as LV dysfunction and cardiomyopathy. Indeed, the level of hyperglycemia achieved in this guinea pig model (~34%) was more akin to what is observed in humans (25–50%) compared with that observed in previous studies reporting marked APD prolongation.

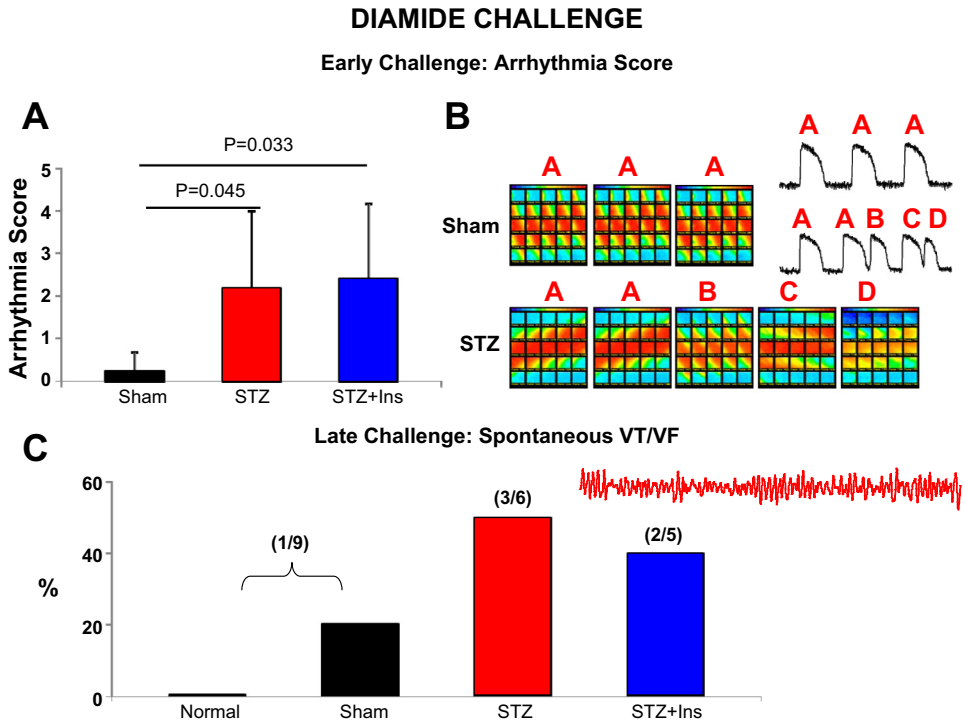

Fig. 6. Enhanced susceptibility of STZ and STZ + Ins hearts to oxidative stress. *A*: assessment of relative sensitivity to early diamide challenge by quantification of a standard ASI during the initial 10-min period of diamide challenge. A marked rise in ASI was observed during the 10-min diamide challenge protocol in STZ and STZ + Ins hearts compared with sham-operated hearts. *B*: representative action potential traces and isopotential contour maps recorded from sham-operated and STZ hearts following early challenge with diamide, showing enhanced susceptibility of STZ hearts to GSH oxidation. While early diamide challenge failed to disrupt steady-state baseline pacing of sham-operated hearts, it caused the generation of triggered beats in STZ hearts. Color bars indicate depolarized myocardium (red) and resting membrane potential (blue). *C*: percentage of hearts in each group (normal, sham-operated, STZ, and STZ + Ins) undergoing sustained VT/VF during a 30-min challenge with diamide perfusion. Normal animals were uninjected. Sham-operated animals were injected with saline buffer.

Finally, we found that guinea pigs with chronic hyperglycemia exhibited a stable rhythm with no change in the QT-interval duration on volume-conducted ECG recordings (sham, 209 ± 10; STZ, 208 ± 17; and STZ + Ins, 209 ± 15 ms). While QT-interval prolongation in patients with t1DM is an important risk factor for sudden death, it is typically uncovered by confounding factors such as ketoacidosis or spontaneous hypoglycemia, known to occur in these patients (37). As such, our finding of preserved APD and QT-interval in the absence of additional pathogenic factors is consistent with stable clinical electrocardiographic properties of patients with t1DM under basal conditions (37).

Conduction Slowing in Chronic Hyperglycemia and its Potential Reversal by Insulin

Conduction abnormalities underlie the initiation and maintenance of reentrant arrhythmias in common structural heart diseases, including ischemia (23), myocardial infarction (44), hypertrophy (21), and heart failure (4, 18, 35). Of interest, Shimoni and colleagues (39) identified conduction changes in hearts of STZ-injected rats. Specifically, they found compelling evidence of reduced conduction reserve in male but not female diabetic rat hearts. These sex-dependent changes in conduction were related to remodeling of the main ventricular gap junction protein, Cx43 in t1DM. Despite these elegant findings, the functional relevance of conduction slowing or reduced conduction reserve in t1DM remained speculative because arrhythmias were not directly provoked in these studies. Therefore, we sought to investigate whether conduction is indeed compromised in this guinea pig model of chronic hyperglycemia and whether it is causally related to arrhythmogenesis. Our finding of minor (<15%) conduction slowing in STZ compared with sham-operated animals is qualitatively similar to that of Nygren et al. (32) who documented the presence of conduction abnormalities in diabetes. However, a major new finding of the present report is the demonstration that despite conduction slowing during baseline normoxic perfusion of the heart, arrhythmia propensity was not altered since challenge of these hearts with PES failed to provoke arrhythmias (Fig. 5*A*). As such, we argue against, not for, a functionally significant role of conduction changes in the setting of chronic hyperglycemia.

Proarrhythmic Triggers and Substrate in Chronic Hyperglycemia

Emerging evidence implicates mitochondrial dysfunction and OS as central features of the diabetic heart (10). Recently, we and others demonstrated strong mechanistic links between mitochondrial dysfunction caused by OS and arrhythmias (1, 7, 9). Whether OS is a required component of the arrhythmia substrate of the diabetic heart remained unknown.

A major finding of the present report is the surprisingly preserved electrical phenotype of hyperglycemic hearts during baseline perfusion. However, upon challenge of hearts with diamide, we uncovered a preferential sensitivity of STZ-injected animals to arrhythmic triggers. Using this strategy, we directly related changes in the EP substrate to the incidence of arrhythmias in the same hearts. We found that diamide-mediated APD shortening was comparable across groups and therefore could not account for differences in arrhythmia vulnerability. Similarly, OS by GSH oxidation did not alter conduction properties or the action potential upstroke before arrhythmia onset (not shown). These findings indicate that exogenous OS in diabetic hearts did not cause arrhythmias by reducing excitability (i.e., promoting "metabolic sink") (1, 2). As such, our current findings argue against surface ATP-sensitive K^+ channel activation driven by mitochondrial membrane potential

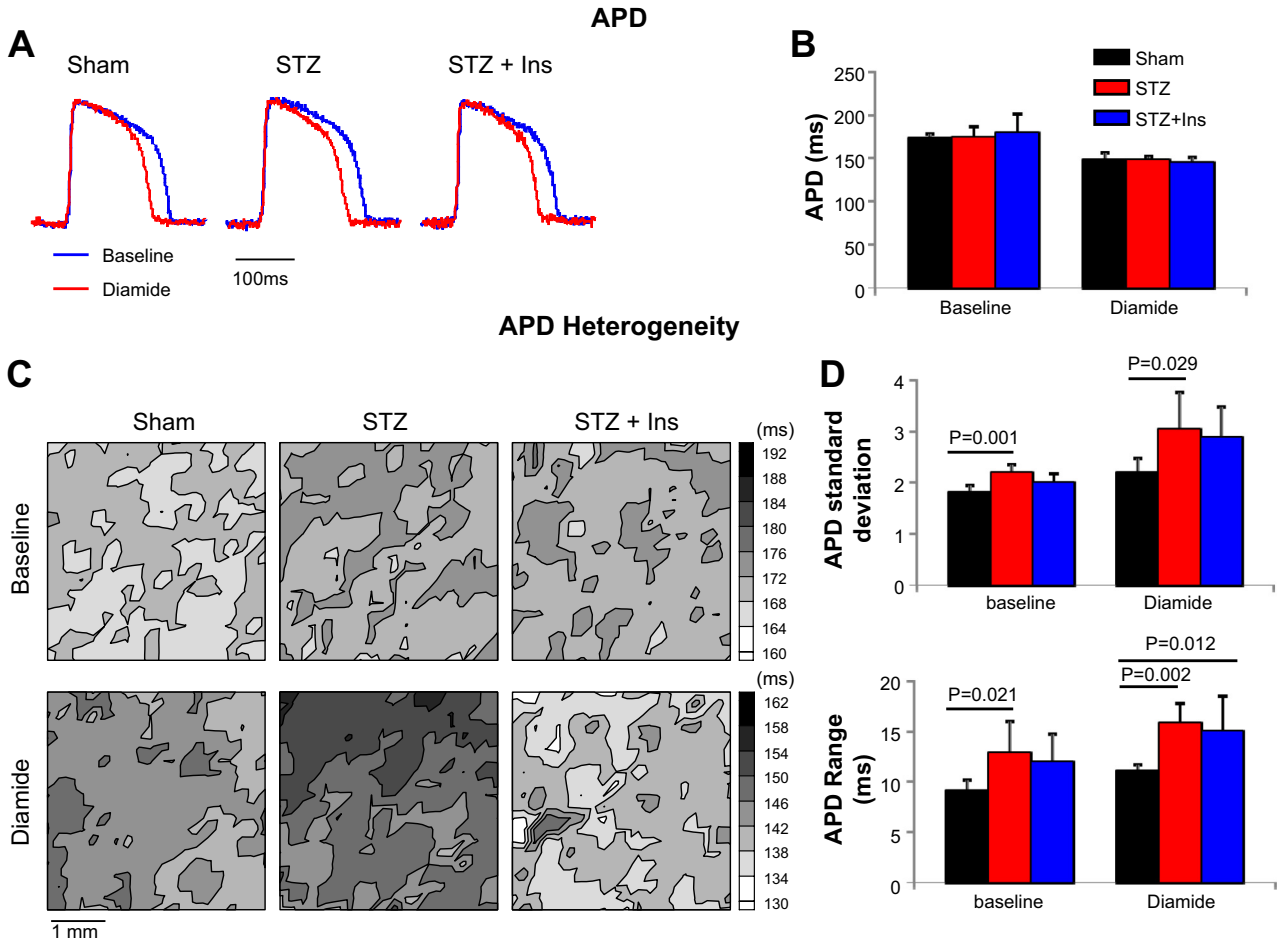

Fig. 7. Diamide-induced changes in APD and APD heterogeneity. *A*: representative action potential traces recorded before and after challenge with diamide (last minute before onset of VT/VF) in sham-operated, STZ, and STZ + Ins hearts. *B*: average APD measured during baseline (*left*) and following diamide challenge (*right*) in sham-operated (*black*), STZ (*red*), and STZ + Ins (*blue*) hearts. *C*: representative APD contour maps measured at baseline and following 10-min challenge with diamide in sham-operated, STZ, and STZ + Ins hearts. *D*: average APD heterogeneity indexed by the standard deviation and range of APD values measured across the mapping field before and after challenge with 200 μM diamide perfusion.

($\Delta\Psi_m$) depolarization as a primary arrhythmia mechanism in chronic hyperglycemia.

Instead, we find that diamide challenge of STZ hearts leads to a marked increase in the spatial heterogeneity of APD (Fig. 7). The exact mechanism underlying this important EP feature remains unknown. However, one may speculate that increased heterogeneity of the mitochondrial $\Delta\Psi_m$ upon diamide perfusion may underlie APD heterogeneities at a microscopic level in these hearts. In support of this hypothesis, Slodzinski et al. (43) used two-photon microscopy to demonstrate that acute OS by GSH oxidation readily produces heterogeneous fluctuations in the mitochondrial $\Delta\Psi_m$ and reactive oxygen species levels between neighboring myocytes within the intact guinea pig heart (43). Since $\Delta\Psi_m$ oscillations can drive APD oscillations (1), spatiotemporal changes in $\Delta\Psi_m$ may indeed increase APD heterogeneity across the heart. Moreover, we have recently

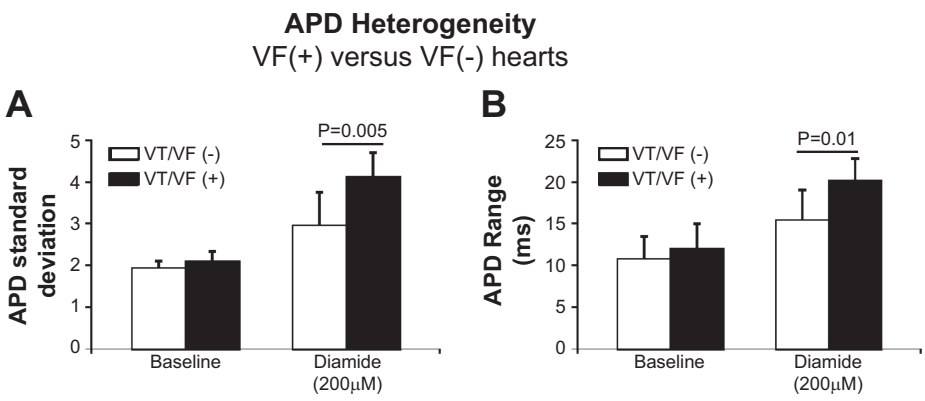

Fig. 8. APD heterogeneity in VT/VF (+) and VT/VF (−) hearts. *A* and *B*: average APD heterogeneity at baseline and following late challenge with diamide in VT/VF (−) and VT/VF (+) hearts. Hearts that exhibited sustained VT/VF within 30 min of diamide perfusion were considered VT/VF (+), whereas those that did not exhibit sustained VT/VF during the same time period were considered VT/VF(−). In VT/VF (+) hearts, APD heterogeneity was computed during the final minute of successful pacing before arrhythmia onset. In VT/VF (−) hearts, APD heterogeneity was computed at the end of the 30-min diamide protocol.

found that increased $\Delta\Psi_m$ heterogeneity is an important feature of hypertrophied hearts, which are highly prone to arrhythmias (22). Further studies are required to uncover the culprit molecular/metabolic mechanisms that underlie increased APD heterogeneity in t1DM and to define their exact role in the genesis of conduction block and arrhythmias.

In addition to APD heterogeneity, we also found that diamide promoted the formation of triggered beats in STZ hearts (Fig. 6). Increased ventricular ectopy in the wake of a spatially heterogeneous repolarizing substrate is consistent with enhanced sensitivity to arrhythmias. The striking finding of diamide-mediated ectopy in STZ is consistent with increased calcium sparks and triggered action potentials observed by Zhou et al. (48) in guinea pig hearts during OS-induced mitochondrial $\Delta\Psi_m$ oscillations.

Finally, a major goal of our current study was to determine whether restoration of blood glucose levels by insulin treatment reverse remodels the EP substrate, decreases the incidence of proarrhythmic triggers, and protects against arrhythmias in chronic hyperglycemia. Surprisingly, we found that despite complete reversal of hyperglycemia (Fig. 2*A*), insulin treatment failed to restore APD heterogeneity (Fig. 7) or to suppress ASI (Fig. 6*A*). These findings indicate that chronic remodeling in hyperglycemia likely involves complex signaling pathways which are not readily reversed by glucose control. Uncovering the signaling cascades that underlie EP remodeling will be essential for the prevention of arrhythmias in t1DM. Our finding that diamide is an effective tool for unmasking arrhythmia propensity in STZ-injected animals suggests that enhancing the reactive oxygen species scavenging capacity of myocytes may indeed be a powerful antiarrhythmic strategy.

Limitations

Our study has several important limitations that require mention. For one, this guinea pig model, which is not associated with weight loss, may not recapitulate key clinical features of human t1DM. Despite achieving a similar percent rise in plasma glucose levels as seen in patients with diabetes, we were careful not to define this as a model of t1DM but rather of chronic hyperglycemia. Moreover, important EP distinctions are known to exist between myocytes from guinea pigs and humans, including presence of a major redox-sensitive repolarizing current (I_{to}) in humans but not guinea pigs.

In our experiments, diamide was used as a prooxidant tool to investigate differences in EP properties between groups under stress conditions. Diamide was specifically chosen because of the established role of GSH depletion in t1DM. It is important to note, however, that ex vivo diamide perfusion is a highly artificial stressor, and therefore caution must be exercised when extrapolating our findings to in vivo OS associated with clinically relevant diseases such as heart failure or ischemia-reperfusion injury.

While our finding of increased APD heterogeneity in VT/VF prone hearts suggests a reentrant mechanism, we did not map the moment of initiation of these spontaneous arrhythmias. Therefore, we cannot be certain that these arrhythmias were initiated by reentrant circuits. Of note, optical mapping performed shortly following the initiation of arrhythmias consistently revealed the presence of wave breaks and reentrant activity (not shown).

Finally, motion artifact was suppressed using electromechanical uncoupling with blebbistatin. Previous studies have found minimal effects of this strategy on key EP properties and arrhythmia propensity compared with other uncoupling agents (15, 27). However, blebbistatin may theoretically alter the response of hearts to diamide. By using an identical concentration of blebbistatin in all our experiments, we ensured that EP differences between groups were not likely due to electromechanical suppression.

ACKNOWLEDGMENTS

This work was supported by National Heart, Lung, and Blood Institute Grant R01-HL-091923-01 and grants from the American Heart Association and the Irma T. Hirschl and Monique Weill Caullier Trusts.

DISCLOSURES

No conflicts of interest, financial or otherwise, are declared by the author(s).

AUTHOR CONTRIBUTIONS

C.X., N.B., C.G.T., M.A.A., and J.K. performed experiments; C.X., N.B., C.G.T., and M.A.A. analyzed data; C.X. and M.A.A. prepared figures; C.X., N.B., C.G.T., M.A.A., N.P., J.K., and F.G.A. approved final version of manuscript; M.A.A., N.P., and F.G.A. edited and revised manuscript; F.G.A. conception and design of research; F.G.A. interpreted results of experiments; F.G.A. drafted manuscript.

REFERENCES

1. **Akar FG, Aon MA, Tomaselli GF, O'Rourke B.** The mitochondrial origin of postischemic arrhythmias. *J Clin Invest* 115: 3527–3535, 2005.
2. **Akar FG, O'Rourke B.** Mitochondria are sources of metabolic sink and arrhythmias. *Pharmacol Ther* 131: 287–294, 2011.
3. **Akar FG, Rosenbaum DS.** Transmural electrophysiological heterogeneities underlying arrhythmogenesis in heart failure. *Circ Res* 93: 638–645, 2003.
4. **Akar FG, Spragg DD, Tunin RS, Kass DA, Tomaselli GF.** Mechanisms underlying conduction slowing and arrhythmogenesis in nonischemic dilated cardiomyopathy. *Circ Res* 95: 717–725, 2004.
5. **Akar FG, Yan GX, Antzelevitch C, Rosenbaum DS.** Unique topographical distribution of M cells underlies reentrant mechanism of torsade de pointes in the long-QT syndrome. *Circulation* 105: 1247–1253, 2002.
6. **Aomine M, Yamato T.** Electrophysiological properties of ventricular muscle obtained from spontaneously diabetic mice. *Exp Anim* 49: 23–33, 2000.
7. **Biary N, Xie C, Kauffman J, Akar FG.** Biophysical properties and functional consequences of reactive oxygen species (ROS)-induced ROS release in intact myocardium. *J Physiol* 589: 5167–5179, 2010.
8. **Brindisi MC, Bouillet B, Verges B, Halimi S.** Cardiovascular complications in type 1 diabetes mellitus. *Diabetes Metab* 36: 341–344, 2010.
9. **Brown DA, Aon MA, Frasier CR, Sloan RC, Maloney AH, Anderson EJ, O'Rourke B.** Cardiac arrhythmias induced by glutathione oxidation can be inhibited by preventing mitochondrial depolarization. *J Mol Cell Cardiol* 48: 673–679, 2010.
10. **Bugger H, Abel ED.** Mitochondria in the diabetic heart. *Cardiovasc Res* 88: 229–240, 2010.
11. **Christensen TF, Tarnow L, Randlov J, Kristensen LE, Struijk JJ, Eldrup E, Hejlesen OK.** QT interval prolongation during spontaneous episodes of hypoglycaemia in type 1 diabetes: the impact of heart rate correction. *Diabetologia* 53: 2036–2041, 2010.
13. **Ding Y, Zou R, Judd RL, Zhong J.** Endothelin-1 receptor blockade prevented the electrophysiological dysfunction in cardiac myocytes of streptozotocin-induced diabetic rats. *Endocrine* 30: 121–127, 2006.

13a. **Dominguez C, Ruiz E, Gussinye M, Carrascosa A.** Oxidative stress at onset and in early stages of type 1 diabetes in children and adolescents. *Diabetes Care* 21: 1736–1742, 1998.

14. **Due-Andersen R, Hoi-Hansen T, Larroude CE, Olsen NV, Kanters JK, Boomsma F, Pedersen-Bjergaard U, Thorsteinsson B.** Cardiac

repolarization during hypoglycaemia in type 1 diabetes: impact of basal renin-angiotensin system activity. *Europace* 10: 860–867, 2008.
15. **Fedorov VV, Lozinsky IT, Sosunov EA, Anyukhovsky EP, Rosen MR, Balke CW, Efimov IR.** Application of blebbistatin as an excitation-contraction uncoupler for electrophysiologic study of rat and rabbit hearts. *Heart Rhythm* 4: 619–626, 2007.
16. **Ghaly H, Boyle P, Vigmond E, Nygren A.** Reduced conduction reserve of the propagating cardiac impulse in the diabetic rat heart: a model study. *Conf Proc IEEE Eng Med Biol Soc* 2008: 5926–5929, 2008.
17. **Giunti S, Bruno G, Lillaz E, Gruden G, Lolli V, Chaturvedi N, Fuller JH, Veglio M, Cavallo-Perin P.** Incidence and risk factors of prolonged QTc interval in type 1 diabetes: the EURODIAB Prospective Complications Study. *Diabetes Care* 30: 2057–2063, 2007.
18. **Glukhov AV, Fedorov VV, Kalish PW, Ravikumar VK, Lou Q, Janks D, Schuessler RB, Moazami N, Efimov IR.** Conduction remodeling in human end-stage nonischemic left ventricular cardiomyopathy. *Circulation* 125: 1835–1847, 2010.
19. **Howarth FC, Chandler NJ, Kharche S, Tellez JO, Greener ID, Yamanushi TT, Billeter R, Boyett MR, Zhang H, Dobrzynski H.** Effects of streptozotocin-induced diabetes on connexin43 mRNA and protein expression in ventricular muscle. *Mol Cell Biochem* 319: 105–114, 2008.
20. **Howarth FC, Jacobson M, Qureshi MA, Shafiullah M, Hameed RS, Zilahi E, Al Haj A, Nowotny N, Adeghate E.** Altered gene expression may underlie prolonged duration of the QT interval and ventricular action potential in streptozotocin-induced diabetic rat heart. *Mol Cell Biochem* 328: 57–65, 2009.
21. **Jin H, Chemaly ER, Lee A, Kho C, Hadri L, Hajjar RJ, Akar FG.** Mechanoelectrical remodeling and arrhythmias during progression of hypertrophy. *FASEB J* 24: 451–463, 2010.
22. **Jin H, Nass RD, Joudrey PJ, Lyon AR, Chemaly ER, Rapti K, Akar FG.** Altered spatiotemporal dynamics of the mitochondrial membrane potential in the hypertrophied heart. *Biophys J* 98: 2063–2071, 2010.
23. **Kleber AG, Janse MJ, Wilms-Schopmann FJ, Wilde AA, Coronel R.** Changes in conduction velocity during acute ischemia in ventricular myocardium of the isolated porcine heart. *Circulation* 73: 189–198, 1986.
24. **Kuppermann N, Park J, Glatter K, Marcin JP, Glaser NS.** Prolonged QT interval corrected for heart rate during diabetic ketoacidosis in children. *Arch Pediatr Adolesc Med* 162: 544–549, 2008.
25. **Lengyel C, Virag L, Biro T, Jost N, Magyar J, Biliczki P, Kocsis E, Skoumal R, Nanasi PP, Toth M, Kecskemeti V, Papp JG, Varro A.** Diabetes mellitus attenuates the repolarization reserve in mammalian heart. *Cardiovasc Res* 73: 512–520, 2007.
25a. **Li S, Li X, Li YL, Shao CH, Bidasee KR, Rozanski GJ.** Insulin regulation of glutathione and contractile phenotype in diabetic rat ventricular myocytes. *Am J Physiol Heart Circ Physiol* 292: H1619–H1629, 2007.
26. **Li X, Xu Z, Li S, Rozanski GJ.** Redox regulation of Ito remodeling in diabetic rat heart. *Am J Physiol Heart Circ Physiol* 288: H1417–H1424, 2005.
27. **Lou Q, Li W, Efimov IR.** The role of dynamic instability and wavelength in arrhythmia maintenance as revealed by panoramic imaging with blebbistatin vs. 2,3-butanedione monoxime. *Am J Physiol Heart Circ Physiol* 302: H262–H269, 2012.
28. **Lyon AR, Joudrey PJ, Jin D, Nass RD, Aon MA, O'Rourke B, Akar FG.** Optical imaging of mitochondrial function uncovers actively propagating waves of mitochondrial membrane potential collapse across intact heart. *J Mol Cell Cardiol* 49: 565–575, 2010.
29. **McNally PG, Lawrence IG, Panerai RB, Weston PJ, Thurston H.** Sudden death in type 1 diabetes. *Diabetes Obes Metab* 1: 151–158, 1999.
31. **Nishiyama A, Ishii DN, Backx PH, Pulford BE, Birks BR, Tamkun MM.** Altered K^+ channel gene expression in diabetic rat ventricle: isoform switching between Kv42 and Kv14. *Am J Physiol Heart Circ Physiol* 281: H1800–H1807, 2001.
32. **Nygren A, Olson ML, Chen KY, Emmett T, Kargacin G, Shimoni Y.** Propagation of the cardiac impulse in the diabetic rat heart: reduced conduction reserve. *J Physiol* 580: 543–560, 2007.
33. **Pacher P, Ungvari Z, Nanasi PP, Kecskemeti V.** Electrophysiological changes in rat ventricular and atrial myocardium at different stages of experimental diabetes. *Acta Physiol Scand* 166: 7–13, 1999.
34. **Pastore A, Ciampalini P, Tozzi G, Pecorelli L, Passarelli C, Bertini E, Piemonte F.** All glutathione forms are depleted in blood of obese and type 1 diabetic children. *Pediatr Diabetes* 13: 272–277. 2010.
35. **Poelzing S, Rosenbaum DS.** Altered connexin43 expression produces arrhythmia substrate in heart failure. *Am J Physiol Heart Circ Physiol* 287: H1762–H1770, 2004.
36. **Raimondi L, De Paoli P, Mannucci E, Lonardo G, Sartiani L, Banchelli G, Pirisino R, Mugelli A, Cerbai E.** Restoration of cardiomyocyte functional properties by angiotensin II receptor blockade in diabetic rats. *Diabetes* 53: 1927–1933, 2004.
37. **Robillon JF, Sadoul JL, Benmerabet S, Joly-Lemoine L, Fredenrich A, Canivet B.** Assessment of cardiac arrhythmic risk in diabetic patients using QT dispersion abnormalities. *Diabetes Metab* 25: 419–423, 1999.
38. **Schlosser MJ, Kapeghian JC, Verlangieri AJ.** Effects of streptozotocin in the male guinea pig: a potential animal model for studying diabetes. *Life Sci* 35: 649–655, 1984.
39. **Shimoni Y, Emmett T, Schmidt R, Nygren A, Kargacin G.** Sex-dependent impairment of cardiac action potential conduction in type 1 diabetic rats. *Am J Physiol Heart Circ Physiol* 296: H1442–H1450, 2009.
40. **Shimoni Y, Ewart HS, Severson D.** Type I and II models of diabetes produce different modifications of K^+ currents in rat heart: role of insulin. *J Physiol* 507: 485–496, 1998.
41. **Shimoni Y, Firek L, Severson D, Giles W.** Short-term diabetes alters K^+ currents in rat ventricular myocytes. *Circ Res* 74: 620–628, 1994.
42. **Sivitz WI, Yorek MA.** Mitochondrial dysfunction in diabetes: from molecular mechanisms to functional significance and therapeutic opportunities. *Antioxid Redox Signal* 12: 537–577, 2010.
43. **Slodzinski MK, Aon MA, O'Rourke B.** Glutathione oxidation as a trigger of mitochondrial depolarization and oscillation in intact hearts. *J Mol Cell Cardiol* 45: 650–660, 2008.
44. **Ursell PC, Gardner PI, Albala A, Fenoglio JJ Jr, Wit AL.** Structural and electrophysiological changes in the epicardial border zone of canine myocardial infarcts during infarct healing. *Circ Res* 56: 436–451, 1985.
45. **Xu Z, Patel KP, Lou MF, Rozanski GJ.** Up-regulation of K^+ channels in diabetic rat ventricular myocytes by insulin and glutathione. *Cardiovasc Res* 53: 80–88, 2002.
46. **Yuill KH, Tosh D, Hancox JC.** Streptozotocin-induced diabetes modulates action potentials and ion channel currents from the rat atrioventricular node. *Exp Physiol* 95: 508–517, 2010.
47. **Zhang Y, Xiao J, Lin H, Luo X, Wang H, Bai Y, Wang J, Zhang H, Yang B, Wang Z.** Ionic mechanisms underlying abnormal QT prolongation and the associated arrhythmias in diabetic rabbits: a role of rapid delayed rectifier K^+ current. *Cell Physiol Biochem* 19: 225–238, 2007.
48. **Zhou L, Aon MA, Liu T, O'Rourke B.** Dynamic modulation of Ca^{2+} sparks by mitochondrial oscillations in isolated guinea pig cardiomyocytes under oxidative stress. *J Mol Cell Cardiol* 51: 632–639, 2010.